An Inductive MEMS Accelerometer

Hadi Tavakkoli[1], Hadi Ghasemzadeh Momen[2], Ebrahim Abbaspour Sani[1], and Metin Yazgi[2]

[1] Microelectronic Research Laboratory, Urmia University, Urmia, Iran
ha.tavakoli@urmia.ac.ir, e.abbaspour@urmia.ac.ir
[2] Istanbul Technical University, Faculty of Electrical and Electronics Engineering, Department of Electronics and Communication Eng., 34469, Maslak, İstanbul, TURKEY
momen@itu.edu.tr, yazgim@itu.edu.tr

Abstract

In this paper, a linear single axis electromagnetic accelerometer with new sensing principle has been proposed. The accelerometer consists of fixed planar spiral inductor that has been sandwiched between two ferromagnetic layers. One of the layers is under the planar coil and the other one is attached to the proof-mass of the accelerometer. The principle of the design is based on the inductance variation due to vertical distance changing between the ferromagnetic layers. The salient feature of the proposed structure is the high dependence of its sensitivity to the ferromagnetic layers thickness and relative permeability. Therefore in a fixed die size the sensitivity can be improved by controlling aforementioned parameters. The advantage of proposed method is that the sensitivity can be increased by using thicker ferromagnetic layers with higher relative permeability which is achievable in micro fabrication without altering the accelerometer layout.

1. Introduction

MEMS accelerometer has widespread application in many domains, such as automotive (airbag deployment and active suspensions), consumer electronics (smart phones and video game consoles) and industrial applications (vehicle tilt monitoring, seismic imaging and oil exploration). The first MEMS accelerometer has been reported in 1979[1]. There are different types of MEMS accelerometers including capacitive [2,3], piezoresistive[4,5], piezoelectric[6], tunneling[7], optical[8,9], thermal[10,11]. Among these types capacitive, piezoresistive, piezoelectric are more popular. Each of these methods has their own advantages and disadvantages in comparison with the others. For example piezoelectric accelerometers are not suitable for static accelerations and capacitive type is more stable for temperature variation than piezoresistive and piezoelectric but it needs more complex interface circuit. The piezoresistive one's circuitry is simpler than the others. According to the application criteria the type of the accelerometer could be determined.

Nowadays wireless sensing of physical phenomena has triggered great enthusiasm in implantable bio-MEMS sensors. In such structures planar inductors can be utilized as sensing element, data and power link [12]. Variable and constant inductors have been employed in strain [13] and pressure sensors [14], respectively. H.C Chang and et al [15] have introduced a pressure sensor which is based on inductance variation due to relative permeability changing. Author has presented electromagnetic accelerometer which is based on the variation of mutual inductance between two planar coils [16].

In this paper a new electromagnetic accelerometer has been proposed which is based on the variation of the self-inductance of sandwiched planar inductor between two ferromagnetic layers. Coil and the ferromagnetic layer which is located under the inductor are fixed and the movable ferromagnetic layer is deposited on the proof mass. As the proof mass is displaced vertically due to exerted acceleration the distance between the two ferromagnetic layers alters, thus the sandwiched coil's self-inductance varies almost linearly in the range of applied acceleration. The proposed structure's figure of merit is that the sensitivity is not only affected by the planar coil's layout parameters but also strongly influenced by the permeability and thickness of the ferromagnetic layers. The higher the thickness and permeability of ferromagnetic layers are, the higher the sensitivity is achieved. Cross axis sensitivity is eliminated by considering the ferromagnetic layers wider than the planar coil in both lateral directions.

2. The theory of work

The proposed structure of the accelerometer is depicted in Fig.1. It consists of a fixed circular planar spiral coil which is sandwiched between two ferromagnetic layers. One of the ferromagnetic layers is beneath the inductor and the other one is attached to the proof mass. The inductance of the coil is highly dependent on the ferromagnetic layers distance [17] which can be changed owing to the exerted acceleration vertically. Hence, the inductance variation determines the amount of the applied acceleration. It is worthy to note that the ferromagnetic layers are designed to be wider than the coil in lateral directions to eliminate the effect of in-plane acceleration on inductance variation.

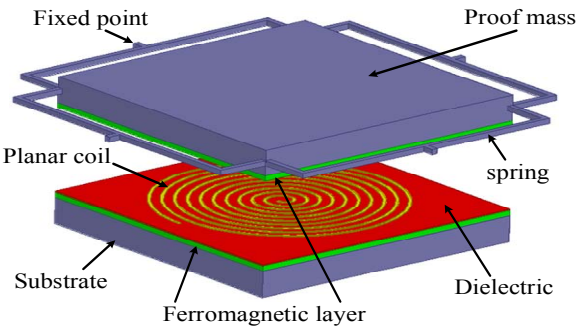

Fig. 1. Arrangement of printing area on an A4 size page for the first and subsequent pages of the manuscript

The inductance of the sandwiched coil can be classified into two parts. The first one is the inductance of the coil in the absence of ferromagnetic layers and the second part is the additional inductance due to the presence of the aforementioned layers. The inductance variation of the proposed accelerometer is just related to the second part. To calculate the inductance of the two aforesaid parts, planar coil is approximated by a set of concentric rings connected in series which has been introduced for the first time in 1980 [18]. Consequently, total inductance (L) of planar coil in Fig.1 can be expressed as following:

$$L = \sum_{i=1}^{N}(L_{i-a} + L_{i-f}) + 2\sum_{j=1}^{N-1}\sum_{k=j+1}^{N}(M_{jk-a} + M_{jk-f}) \quad (1)$$

Where Li-f , Li-a are the self-inductance of ith turn and Mjk-f , Mjk-a are the mutual inductance between ith and jth turns with and without ferromagnetic layers, respectively. So, to evaluate the Eq. (1) the concentric rings' self and mutual inductances have to be examined.

Many literatures have been published for the calculation of mutual inductance between two rings in the air [19, 20, 21]. The mutual inductance between two rings in same plane with identical thickness (h) as shown in Fig.2, is formulated as [22]:

$$M = \frac{\mu_0 \pi}{h^2 \ln(\frac{r_2}{r_1}) \ln(\frac{a_2}{a_1})} \int_0^{\infty} S(kr_2, kr_1) S(ka_2, ka_1) \frac{2}{k}\left(h + \frac{e^{-kh}-1}{k}\right) dk \quad (2)$$

Where μ_0 is the permeability of the free space, a1, a2, r1, r2 and h are rings dimensions which are displayed in Fig. 2 and the S function is defined in Eq. (3). It is noteworthy, in equation (2), non-uniformity of distributed current across the widths of the rings has been taken into account.

$$S(kx, ky) = \frac{J_0(kx) - J_0(ky)}{k} \quad (3)$$

Where J0 is the Bessel functions of the first kind. According to Eq. 2 the self-inductance e.g. outer ring in Fig. 2, is written as:

$$L_s = \frac{\mu_0 \pi}{(h \times \ln(\frac{r_2}{r_1}))^2} \int_0^{\infty} (S(kr_2, kr_1))^2 \times \left(\frac{2}{k}\left(h + \frac{e^{-kh}-1}{k}\right)\right) dk \quad (4)$$

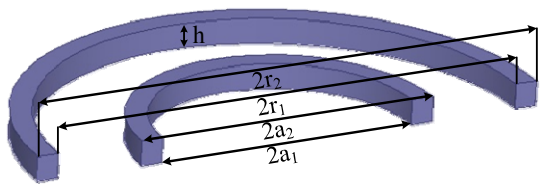

Fig. 2. Cross section view of two circular rings in air

Analytical solution of Eq. (2&4) seems relatively difficult; however, it is completely amenable to numerical approach. Geometric mean distance method [23] can be used instead of Eq. (2) which demands less computational efforts.

In [24] the image method has been exploited to study the inductance of sandwiched circular planar coils between two infinite thickness ferromagnetic layers. However, this method is simple in the case of infinite thickness ferromagnetic layers but in the matter of finite thickness it is very sophisticated.

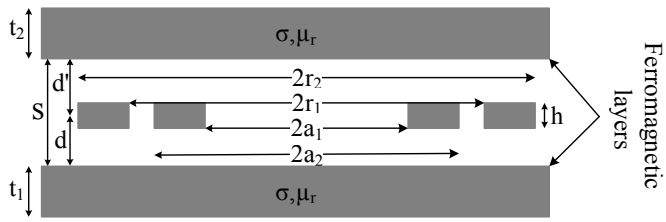

Fig. 3. Cross section of two coils sandwiched between two ferromagnetic layers

W.G. Hurley et al [25] have solved Maxwell equations for finite thickness ferromagnetic layers, which is employed in this work. The additional mutual inductance due to presence of ferromagnetic layers (Fig. 3) is as following:

$$M_f = Real\left(\frac{\mu_0 \pi}{h^2 \ln\left(\frac{r_2}{r_1}\right) \ln\left(\frac{a_2}{a_1}\right)} \int_0^{\infty} S(kr_2, kr_1) S(ka_2, ka_1) \frac{2}{k}\left(h + \frac{e^{-kh}-1}{k}\right)\left(f(\lambda) + g(\lambda)\right)\right) dk \quad (5)$$

Where s, d, d', a1, a2, r1, r2 and h are illustrated in Fig. 3.

$$f(\lambda) = \frac{\lambda(t_1)e^{-2kd} + \lambda(t_2)e^{-2kd'}}{1 - \lambda(t_1)\lambda(t_2)e^{-2ks}} \quad (6)$$

$$g(\lambda) = \frac{2\lambda(t_1)\lambda(t_2)e^{-2ks}}{1 - \lambda(t_1)\lambda(t_2)e^{-2ks}} \quad (7)$$

$$\lambda(t) = \phi(k)\frac{1 - e^{-2\eta t}}{1 - \phi(k)^2 e^{-2\eta t}} \quad (8)$$

$$\phi(k) = \frac{\mu_r - \frac{\eta}{k}}{\mu_r + \frac{\eta}{k}} \quad (9)$$

$$\eta = \sqrt{k^2 + j\omega\mu_r\mu_0\sigma} \quad (10)$$

Where $\omega = 2\pi f$ and f denotes the frequency in Hz, μr and σ are relative permeability and conductivity of the ferromagnetic layers, respectively.

2. Accelerometer design

Regarding section II variable sandwiched inductor has been utilized in the proposed accelerometer. With respect to Eq. (1), (2) & (5), seven parameters which affect the sensitivity of the proposed accelerometer, have to be determined in the design of the sandwiched inductor. Two of these parameters are related to ferromagnetic layers, which are thickness (t) and relative permeability (μr) of the ferromagnetic layers. Five remaining parameters are N, W, S, H and Do that denotes to number of turns, tracks' width, spacing between two adjacent tracks, thickness of coil and outer diameter of the inductor, respectively. The effect of the aforementioned parameters on the performance of the accelerometer, in fixed outer diameter of the coil (700 µm), is discussed in this section. The outer diameter of the coil is related to the coil parameters as following:

$$D_o = D_{in} + 2(N \times W + (N-1) \times S) \quad (15)$$

Where, Din is the inner diameter of the coil. The Minimum Feature Size (MFS) in case of fabricating the device, is considered to be 1µm and initial distance between movable ferromagnetic layer and planar coil is 2.2 µm and maximum displacement of the proof mass in z direction is ±2µm.

The influence of the parameters on the variation of sandwiched coil inductance due to the vertical displacement of movable ferromagnetic layer is studied in four different cases:

3.1. Case 1

In this case variable parameters are number of turns (N) and spacing between tracks (S) of coil. The rest are: thickness of the ferromagnetic layers (t) =1 µm, permeability of ferromagnetic layers (µr) =1000, width of coil's tracks (W) =5µm, thickness of coil's tracks (H) =2 µm. It is worthy to note that Permalloy film with t=1µm, µr=1000 has been reported in [26]. According to Eq. (15) S and N are inversely related to each other in fixed outer diameter of the coil. The effect of aforesaid parameters variation on inductance value in the applied acceleration range is depicted in Fig. 4.

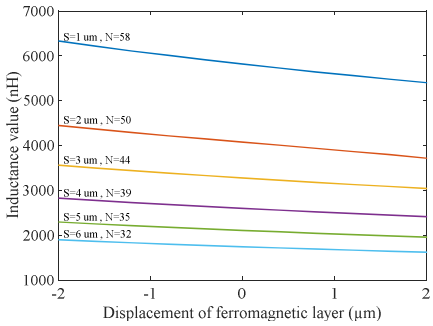

Fig. 4. Inductance variation for different N & S due to ferromagnetic layer displacement with tracks width (W) =5

As it can be concluded from Fig. 4, increasing the spacing between tracks decreases the inductance variation per specified displacement of ferromagnetic layer. Accordingly, S has to be set to its minimum value which is allowed by fabrication process which results in increasing N.

3.3. Case 2

Similar to previous case there are just two variable parameters in this case (N&W) and the remaining parameters are: t=1 µm, µr=1000, S=1 µm and H=2 µm. The inductance variation for different N&W values is displayed in Fig. 6.

It is evident that the smaller W is employed, the more N is obtained. Consequently, higher range of inductance variation is achieved as depicted on Fig. 5. On the other hand, increasing N leads to narrower and longer track. Hence, the DC resistance of the inductor increase which is undesirable in processing circuit. So, there is a tradeoff between The DC resistance and inductance variation. With respect to the processing circuit, optimum case has to be chosen.

3.4. Case 3

The effect of ferromagnetic layer thickness has been probed in this case (Fig. 6) by considering: µr=1000, N=58, W=5, S=1 µm and H=2 µm. According to Fig. 6, by increasing the thickness of ferromagnetic layers, inductance variation enhancement is achieved without affecting the DC resistance of the inductor.

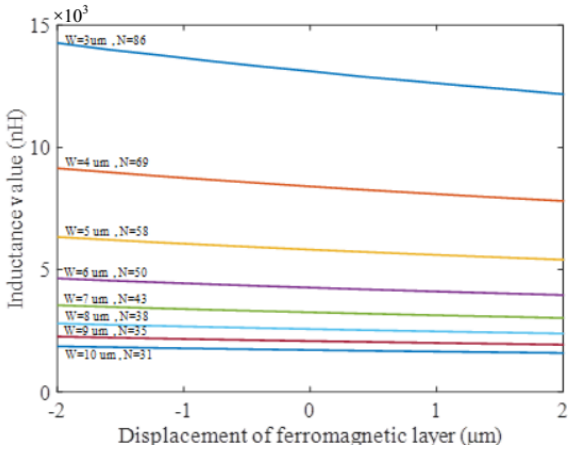

Fig. 5. Inductance variation for different W & N due to ferromagnetic layer displacement

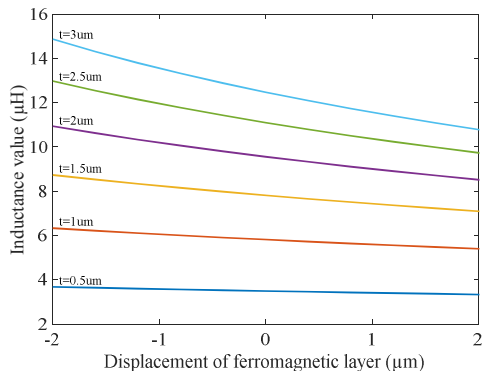

Fig. 6. Inductance variation for different t due to ferromagnetic layer displacement

3.5. Case 4

Permeability of ferromagnetic layers' influence on performance of the proposed structure is shown in Fig. 7. While other parameters are set as following: t=1 µm, N=58, W=5, S=1 µm and H=2 µm.

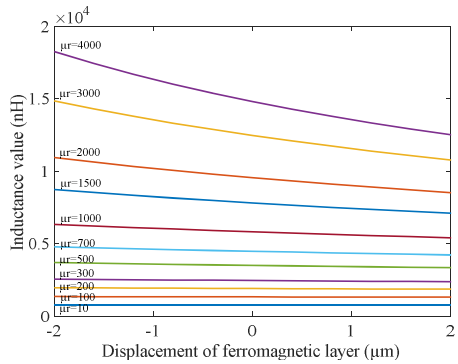

Fig. 7. Inductance variation for different μ_r due to ferromagnetic layer displacement

As it can be comprehended from Fig. 7, increasing permeability of the ferromagnetic layers results in higher sensitivity of the accelerometer.

In cases 1 and 2, the sensitivity enhancement affects the DC resistance of the coil and there is tradeoff between sensitivity and DC resistance. But in cases 3&4 the sensitivity can be improved by increasing the thickness and permeability of ferromagnetic layers without altering the coil resistance, which is the salient feature of the proposed accelerometer.

Performance of the proposed accelerometer is not only influenced by the spiral planar coil layout parameters, but also it is strongly related to the thickness and relative permeability of the ferromagnetic layers. The effect of coil's layout and ferromagnetic layers parameters on the sensitivity is investigated in previous section. With regard to mentioned cases in a given outer diameter of the coil for higher sensitivity the following results are obtained:

- Spacing between tracks has to set to the minimum feature size of fabrication process (which is considered to be 1 µm in this paper).
- Number of turns and tracks' width are inversely related, increasing number of turns leads to higher inductance variation range in the cost of increasing DC resistance of the coil. Therefore, there is a tradeoff between N and W. According to Fig. 5, moderate circumstance (i.e. W=5 and N=58) has been used in the accelerometer design.
- Due to case 3&4, increasing thickness and relative permeability of the ferromagnetic layers enhances the performance of the sensor. Achieving very high thickness and relative permeability is not amenable in fabrication. CoFeB and Permalloy ferromagnetic films with µr=1382, t=0.2 µm and µr=1000, t=1 µm have been reported in [15] and [26], respectively. In spite of lower relative permeability, Permalloy layer has been utilized in this work due to its five times higher thickness in comparison with CoFeB film.

Table 1 summarizes characterizations of the proposed accelerometer. The ferromagnetic layers dimensions are wider than outer diameter of the coil in both lateral directions. Hence, misalignment during fabrication process and lateral acceleration do not affect the inductance value.

Table 1. characterization of proposed accelerometer

1 blank line using 6-point font with single spacing

Proof mass dimensions	800µm×800 µm×500 µm
Spring constant z direction	182.515
Maximum displacement (at 50g)	2 µm
Initial air gap	2.2 µm
Number of turns of coils	58
Track width	5 µm
Spacing between tracks	1 µm
Outer diameter of coil	700 µm
Track thickness	2 µm
Ferromagnetic layers thickness	1 µm
Ferromagnetic layers relative permeability	1000
Sensitivity	9.285 nH/g
Maximum nonlinearity	3.4 percent
Total die size	950µm×950µm

In Fig. 8 mechanical simulation result for 50 g acceleration has been illustrated. Fig. 9 declares that spring constant does not vary in the range of applied acceleration (±50 g). Inductance variation in the range of exerted acceleration (±50g) is depicted in Fig. 10. Inductance value changes almost linearly with resolution of 9.285 nH/g. The maximum nonlinearity is 3.4 percent.

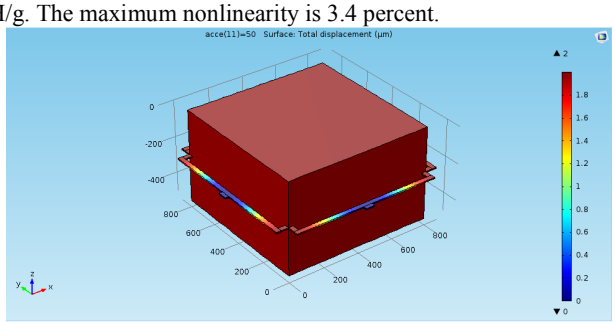

Fig. 8. displacement of proof mass at 50g acceleration

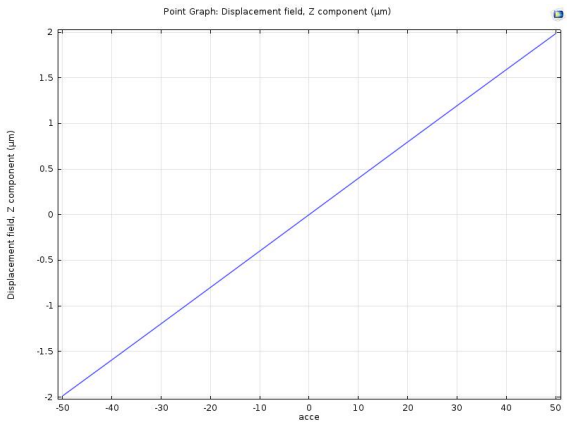

Fig. 9. displacement of proof mass for the applied acceleration between -50g to at 50g

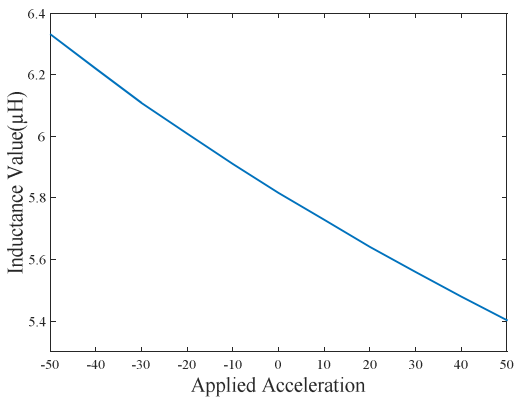

Fig. 10. Inductance variation in the range of applied acceleration ±50g

3. Conclusion

In this paper, a new Z-axis electromagnetic accelerometer with new sensing principle was proposed. The variable sandwich-type ferromagnetic planar inductor was utilized to determine the applied acceleration. One of the ferromagnetic layers is attached to proof mass and the other one is fixed beneath the planar coil. The proof mass displacement in vertical direction leads to

distance variation between two aforementioned layers which results in almost linear inductance variation. The sensitivity of the accelerometer is significantly influenced by ferromagnetic layers' thickness and relative permeability. The inductance variation of 9.2 nH/g was accomplished in the range of ±50g and the total die size of the accelerometer is 950µm×950µm. Higher sensitivity is achievable with higher thickness and relative permeability of ferromagnetic films without altering the layout of accelerometer.

7. References

[1] L.M. Roylance and J.B. Angell, "A batch-fabricated silicon accelerometer", IEEE Trans. Electron Devices, ED-26 (1979) 1911-1917.

[2] M. Mehran, S. Mohajerzadeh, High sensitivity nanostructure incorporated interdigital silicon based capacitive accelerometer, Microelectronics Journal, Volume 46, Issue 2, February 2015, Pages 166-173.

[3] W Qu, C Wenzel, K Drescher, A vertically sensitive accelerometer and its realisation by depth UV lithography supported electroplating, Microelectronics Journal, Volume 31, Issue 7, 30 July 2000, Pages 569-575.

[4] S. Kal, S. Das, D.K. Maurya, K. Biswas, A. Ravi Sankar, S.K. Lahiri, CMOS compatible bulk micromachined silicon piezoresistive accelerometer with low off-axis sensitivity, Microelectronics Journal, Volume 37, Issue 1, January 2006, Pages 22-30.

[5] Yongliang Yang, Wei Jiang, Kun Zhang, Min Liu, Xinxin Li, A dynamic collision model for improved over-range protection of cantilever-mass micromechanical accelerometers, Microelectronics Journal, Volume 41, Issue 6, June 2010, Pages 331-337.

[6] Yu J-C, Lee C, Kuo W, Chang C (2011) "Modeling analysis of a triaxial microaccelerometer with piezoelectric thin-film sensing using energy method." Microsyst Technol 17(4):483–493.

[7] Cheng-Hsien Liu; Kenny, T.W., "A high-precision, wide-bandwidth micromachined tunneling accelerometer," in Microelectromechanical Systems, Journal of , vol.10, no.3, pp.425-433, Sep 2001.

[8] S. J. Lee and D. W. Cho, "Development of micro-opto-mechanical accelerometer based on intensity modulation", Microsyst. Tech. J., vol. 10, pp. 147-154, 2004.

[9] E. Abbaspour-Sani , R.-S. Huang and C. Y. Kwok, "A wide-range linear optical accelerometer", Sens. Actuators A: Phys., vol. 49, no. 3, pp. 149-154, 1995.

[10] B. Mezghani, F. Tounsi, A.A. Rekik, F. Mailly, M. Masmoudi, P. Nouet, Sensitivity and power modeling of CMOS mems single axis convective accelerometers, Microelectronics Journal, Volume 44, Issue 12, December 2013, Pages 1092-1098.

[11] F. Mailly, A. Martinez, A. Giani, F. Pascal-Delannoy, A. Boyer, Design of a micromachined thermal accelerometer: thermal simulation and experimental results, Microelectronics Journal, Volume 34, Issue 4, April 2003, Pages 275-280.

[12] Wu. J, Zhao. C., Du. J, Lin. Z, Hu. Y and He. X., "Wireless Power and Data Transfer via a Common Inductive Link using Frequency Division multiplexing ", Industrial Electronics, IEEE Transactions on. 09 July 2015.

[13] YongAn Huang, Wentao Dong, Tao Huang, Yezhou Wang, Lin Xiaoa,Yewang Su and Zhouping Yin, "Self-similar design for stretchable wireless LC strain sensors", Sensors and Actuators A 224 (2015) 36–42.

[14] J. Xiong, Y. Li, Y. Hong, et al., "Wireless LTCC-based capacitive pressure sensorfor harsh environment", Sens. Actuators A: Phys. 197 (2013) 30–37.

[15] Heng-Chung Chang, Sheng-Chieh Liao, Hsieh-Shen Hsieh, Jung-Hung Wen,Chih-Huang Lai and Weileun Fang, "Magnetostrictive type inductive sensing pressure sensor", Sensors and Actuators A 238 (2016) 25–36.

[16] E. Abbaspour-Sani , R. S. Huang and C. Y. Kwok, "A linear electromagnetic accelerometer", Sens. Actuator A, Phys., vol. 44, pp. 103-109, 1994.

[17] W. G. Hurley and M. C. Duffy, "Calculation of self- and mutual impedances in planar sandwich inductors", in IEEE Transactions on Magnetics, vol. 33, no. 3, pp. 2282-2290, May 1997.

[18] R. Rodriguez, J. Dishman, F. Dickens and E. Whelan, "Modeling of Two-Dimensional Spiral Inductors", in *IEEE Transactions on Components, Hybrids, and Manufacturing Technology*, vol. 3, no. 4, pp. 535-541, Dec 1980.

[19] Babic, S.I. and Akyel, C., "New analytic-numerical solutions for the mutual inductance of two coaxial circular coils with rectangular cross section in air," in Magnetics, IEEE Transactions on , vol.42, no.6, pp.1661-1669, June 2006.

[20] Akyel, C.; Babic, S. and Kincic, S., "New and fast procedures for calculating the mutual inductance of coaxial circular coils (circular coil-disk coil)", in Magnetics, IEEE Transactions on, vol.38, no.5, pp.2367-2369, Sep 2002.

[21] F. W. Grover, "Inductance Calculations", New York: Dover, 1964, ch. 2 and 13.

[22] W. G. Hurley and M. C. Duffy, "Calculation of self and mutual impedances in planar magnetic structures," in IEEE Transactions on Magnetics, vol. 31, no. 4, pp. 2416-2422, Jul 1995.

[23] F. W. Grover, "Inductance Calculations: Working Formulas and Tables", New York: Dover Publications. 1946.

[24] W. A. Roshen, "Analysis of planar sandwich inductors by current images," in IEEE Transactions on Magnetics, vol. 26, no. 5, pp. 2880-2887, Sep 1990.

[25] W. G. Hurley, M. C. Duffy, S. O'Reilly and S. C. O'Mathuna, "Impedance formulas for planar magnetic structures with spiral windings," in IEEE Transactions on Industrial Electronics, vol. 46, no. 2, pp. 271-278, Apr 1999.

[26] V. Korenivski and R. B. van Dover, "Magnetic film inductors for radio frequency applications", J. Appl. Phys., vol. 82, pp. 5247-5254, 1997.